Meteoritics & Planetary Science 35, 1127-1141 (2000)

A petrologic study of the IAB iron meteorites: Constraints on the formation of the IAB–Winonaite parent body

G. K. BENEDIX[1,2*†], T. J. McCOY[3], K. KEIL[1‡] AND S. G. LOVE[4]

[1]Hawaii Institute of Geophysics and Planetology, School of Ocean and Earth Science and Technology, University of Hawaii at Manoa, Honolulu, Hawaii 96822, USA
[2]Arizona State University, Department of Geology, Tempe, Arizona 85287-1404, USA
[3]Department of Mineral Sciences, National Museum of Natural History, Smithsonian Institution, Washington D.C. 20560-0119, USA
[4]Mail Code CB, NASA Johnson Space Center, 2101 NASA Road 1, Houston, Texas 77058, USA
[†]Present address: Department of Geological Sciences, Virginia Tech, Blacksburg, Virginia 24061-0420, USA
[‡]Also associated with the Hawaii Center for Volcanology.
*Correspondence author's e-mail address: gbenedix@vt.edu

(Received 1999 August 3; accepted in revised form 2000 June 6)

Abstract–We studied 26 IAB iron meteorites containing silicate-bearing inclusions to better constrain the many diverse hypotheses for the formation of this complex group. These meteorites contain inclusions that fall broadly into five types: (1) sulfide-rich, composed primarily of troilite and containing abundant embedded silicates; (2) nonchondritic, silicate-rich, comprised of basaltic, troctolitic, and peridotitic mineralogies; (3) angular, chondritic silicate-rich, the most common type, with approximately chondritic mineralogy and most closely resembling the winonaites in composition and texture; (4) rounded, often graphite-rich assemblages that sometimes contain silicates; and (5) phosphate-bearing inclusions with phosphates generally found in contact with the metallic host. Similarities in mineralogy and mineral and O-isotopic compositions suggest that IAB iron and winonaite meteorites are from the same parent body.

We propose a hypothesis for the origin of IAB iron meteorites that combines some aspects of previous formation models for these meteorites. We suggest that the precursor parent body was chondritic, although unlike any known chondrite group. Metamorphism, partial melting, and incomplete differentiation (*i.e.*, incomplete separation of melt from residue) produced metallic, sulfide-rich and silicate partial melts (portions of which may have crystallized prior to the mixing event), as well as metamorphosed chondritic materials and residues. Catastrophic impact breakup and reassembly of the debris while near the peak temperature mixed materials from various depths into the re-accreted parent body. Thus, molten metal from depth was mixed with near-surface silicate rock, resulting in the formation of silicate-rich IAB iron and winonaite meteorites. Results of smoothed particle hydrodynamic model calculations support the feasibility of such a mixing mechanism. Not all of the metal melt bodies were mixed with silicate materials during this impact and reaccretion event, and these are now represented by silicate-free IAB iron meteorites. Ages of silicate inclusions and winonaites of 4.40–4.54 Ga indicate this entire process occurred early in solar system history.

INTRODUCTION

Of the 13 iron meteorite groups, only IAB and IIICD meteorites consist of metal of highly variable Ni composition and commonly contain abundant silicate inclusions. Most of the inclusions are roughly chondritic in mineralogy and composition but have nonchondritic, recrystallized textures and are similar to the stony winonaites in O-isotopic (Clayton and Mayeda, 1996) and mineral compositions (Bild, 1977). The seemingly contradictory presence of relatively primitive silicate inclusions embedded in dense metal that was presumably molten at the time of mixing has led to two main models for their formation. Choi *et al.* (1995) suggested formation by impact-induced large-scale selective melting and mixing in the megaregoliths on a chondritic parent body, whereas Kracher (1982, 1985) suggested formation by parent-body-wide partial melting and fractional crystallization during formation of a S-rich core. Another model proposed to explain the mineralogical and textural features is inhomogenous segregation of silicates and metal (Takeda *et al.*, 1994, 2000; Yugami *et al.*, 1998).

In a recent systematic study of winonaite meteorites, Benedix *et al.* (1998) found petrologic, textural, and isotopic evidence suggesting their formation from heterogeneous chondritic precursor materials by partial melting, brecciation, and metamorphism. The IAB iron meteorites have been more extensively studied than the related winonaite meteorites. The features of the metallic phases were described in detail by Buchwald (1975). Bunch *et al.* (1970) summarized the features of the silicate inclusions in IAB iron meteorites known at that time and Wasson *et al.* (1980) and Choi *et al.* (1995) revisited the history of these meteorites, deduced from study of the metallic hosts. Additional work (*e.g.*, Scott and Bild, 1974; Takeda *et al.*, 1993; Olsen and Schwade, 1998) on silicate inclusions in IAB iron meteorites recovered since the work of Bunch *et al.* (1970) expanded the range of inclusion types. We examined ~40 inclusions in 26 IAB meteorites with the goals of presenting an overview of the range of inclusion types (drawing heavily on details from previous workers) and of examining existing models for the genesis of these meteorites to explain this range of inclusions. In this paper, we present the details of a hybrid model, first suggested by Benedix *et al.* (1996) in abstract form, for the formation of the IAB iron and stony winonaite meteorites that combines the best features of previous models.

SAMPLES AND ANALYTICAL TECHNIQUES

We studied a suite of silicate-bearing IAB iron meteorites (Table 1) including, in some cases, multiple samples of the same meteorite to document the range of inclusion heterogeneity.

TABLE 1. List and sources of IAB iron meteorites reported on in this study.

Meteorite	Section	Source
Caddo County	UNM 927 (Metal)	University of New Mexico
	UNM 937 (Silicate)	University of New Mexico
Campo del Cielo	USNM 5615-1	Smithsonian Institution
	USNM 5615-2	Smithsonian Institution
	USNM 5615-4	Smithsonian Institution
	USNM 5615-6	Smithsonian Institution
	USNM 5615-8	Smithsonian Institution
	USNM 5615-9	Smithsonian Institution
Copiapo	USNM 3204-2	Smithsonian Institution
	USNM 3204-1	Smithsonian Institution
EET 83333	PS	Smithsonian Institution/MWG
EET 84300	PS	Smithsonian Institution/MWG
EET 87505*	EET 87505,4	MWG
EET 87504*	EET 87504,5	MWG
EET 87506*	PTS	Smithsonian Institution/MWG
Four Corners	USNM 728	Smithsonian Institution
Kendall County	USNM 343 (PTS)	Smithsonian Institution
	USNM 1657	Smithsonian Institution
Landes	UH 147	University of Hawaii
Linwood	USNM 1416	Smithsonian Institution
Lueders	UH 255 (Metal-sil)	University of Hawaii
	UH 245 (Silicate)	University of Hawaii
Mundrabilla	USNM 5914-1	Smithsonian Institution
Ocotillo	UH 226	University of Hawaii
Odessa	UH 256	University of Hawaii
	USNM 1418	Smithsonian Institution
Persimmon Creek	USNM 2990	Smithsonian Institution
Pine River	PS	Smithsonian Institution
Pitts	USNM 1378	Smithsonian Institution
San Cristobal	thick section	UC Los Angeles
	USNM 3037a	Smithsonian Institution
Tacubaya†	M201	Texas Christian University
TIL 91725	–	Smithsonian Institution
Toluca†	M8.53	Texas Christian University
	M8.79	Texas Christian University
	M8.150-1	Texas Christian University
	M8.150-2	Texas Christian University
	USNM 931	Smithsonian Institution
Udei Station	USNM 2577	Smithsonian Institution
Woodbine	USNM 2169	Smithsonian Institution
Zagora	USNM 6392	Smithsonian Institution

MWG = Meteorite Working Group.
PS = Polished section.
*EET 87504/5/6 are paired (*Antarctic Meteorite Newsletter*, 1988).
†Toluca and Tacubaya are paired (Scott and Wasson, 1975).

Polished sections and polished thin sections were studied optically. Representative analyses of silicate inclusions in Caddo County, Ocotillo, TIL 91725, and Zagora were determined with a Cameca SX-50 electron microprobe (Table 2). For analyses of mafic minerals, we used a fully focused beam of 15 keV accelerating voltage and 20 nA current. The beam was rastered over a 10 × 10 μm area for plagioclase analyses. Well-known mineral standards were used and data were corrected using a manufacturer-supplied PAP ZAF routine.

DESCRIPTION OF IAB INCLUSIONS

The silicate-bearing IAB iron meteorites span the range of structural classifications from hexahedrites (*e.g.*, Kendall County with 5.5% Ni) through ataxites (*e.g.*, San Cristobal with 24.9% Ni). The textures of the metal phases of IAB iron meteorites have been described previously (*e.g.*, Buchwald, 1975) and those details will not be repeated here. The silicate inclusions typically contain low-Ca

TABLE 2. Compositions (in wt%) of silicates from inclusions in IAB iron meteorites analyzed in this work.

	Olivine*				Orthopyroxene*				Clinopyroxene*				Plagioclase*			
	Caddo County		Ocotillo		Caddo County		Ocotillo		Caddo County		Ocotillo		Caddo County		Ocotillo	
SiO_2	41.59	*0.11*	41.55	*0.49*	57.07	*0.03*	57.83	*0.10*	54.52	*0.16*	54.19	*0.40*	64.23	*0.40*	64.66	*0.50*
TiO_2	n.d.	–	n.d.	–	0.19	*0.02*	0.22	*0.02*	0.69	*0.09*	0.73	*0.06*	n.d.	–	n.d.	–
Al_2O_3	n.d.	–	n.d.	–	0.26	*0.02*	0.22	*0.02*	0.77	*0.03*	0.80	*0.09*	22.81	*0.31*	22.32	*0.42*
Cr_2O_3	n.d.	–	n.d.	–	0.33	*0.02*	0.29	*0.02*	0.62	*0.23*	1.15	*0.16*	n.d.	–	n.d.	–
FeO	2.80	*0.25*	3.35	*0.38*	4.56	*0.07*	4.15	*0.17*	4.61	*0.31*	1.74	*0.17*	b.d.	–	0.21	*0.17*
MnO	0.31	*0.01*	0.33	*0.02*	0.42	*0.01*	0.37	*0.01*	0.32	*0.02*	0.23	*0.03*	b.d.	–	b.d.	–
MgO	54.8	*0.26*	54.3	*0.60*	36.28	*0.19*	36.95	*0.27*	35.49	*0.42*	18.61	*0.14*	18.06	*0.24*	n.d.	–
CaO	b.d.	–	b.d.	–	1.03	*0.13*	0.83	*0.17*	0.89	*0.14*	21.76	*0.22*	22.08	*0.31*	3.40	*0.37*
Na_2O	n.d.	–	n.d.	–	b.d.	–	b.d.	–	b.d.	–	0.75	*0.07*	0.71	*0.10*	9.33	*0.20*
K_2O	n.d.	–	n.d.	–	n.d.	–	n.d.	–	n.d.	–	n.d.	–	n.d.	–	0.59	*0.07*
Total	99.5		99.5		100.8		100.9		99.9		100.0		100.6		100.4	
n	5		15		5		5		11		7		9		14	
Fa	2.8		3.4		–		–		–		–		–		–	
Fs	–		–		6.5		5.8		2.5		3.8		2.9		–	
Wo	–		–		1.9		1.5		43.3		44.4		45.4		–	
An	–		–		–		–		–		–		–		16.2	
Or	–		–		–		–		–		–		–		3.3	

	Olivine*				Orthopyroxene*				Clinopyroxene*				Plagioclase*			
	TIL 91725		Zagora		TIL 91725		Zagora		TIL 91725		Zagora					
SiO_2	42.07	*0.13*	41.88	*0.22*	57.07	*0.03*	58.75	*0.14*	55.1	*0.27*	55.32	*0.23*				
TiO_2	n.d.	–	n.d.	–	0.19	*0.02*	0.26	*0.05*	0.58	*0.04*	0.69	*0.13*				
Al_2O_3	n.d.	–	n.d.	–	0.26	*0.02*	0.22	*0.05*	1.00	*0.10*	0.83	*0.16*				
Cr_2O_3	n.d.	–	n.d.	–	0.33	*0.02*	0.13	*0.02*	1.32	*0.12*	0.92	*0.28*				
FeO	4.41	*0.25*	4.69	*0.11*	4.56	*0.07*	4.61	*0.31*	1.93	*0.10*	1.80	*0.15*				
MnO	0.38	*0.01*	0.26	*0.01*	0.42	*0.01*	0.32	*0.02*	0.26	*0.02*	0.22	*0.04*				
MgO	53.4	*0.21*	53.5	*0.15*	36.28	*0.19*	35.49	*0.42*	17.70	*0.10*	18.06	*0.24*				
CaO	b.d.	–	b.d.	–	1.03	*0.13*	0.89	*0.14*	21.64	*0.16*	22.08	*0.31*				
Na_2O	n.d.	–	n.d.	–	b.d.	–	b.d.	–	0.81	*0.05*	0.71	*0.10*				
K_2O	n.d.	–	n.d.	–	n.d.	–	n.d.	–	n.d.	–	n.d.	–				
Total	100.3		100.4		100.8		100.7		100.4		100.6					
n	11		12		5		15		13		9					
Fa	4.4		4.7		–		–		–		–					
Fs	–		–		6.5		6.7		3.2		2.9					
Wo	–		–		1.9		1.7		45.3		45.4					
An	–		–		–		–		–		–					
Or	–		–		–		–		–		–					

n = number of analyses; b.d. = below detection limit; n.d. = not determined. Formulae endmembers are in mol%.
*italicized figures are 1σ of the compositional variability.

TABLE 3. Summary of petrologic and isotopic characteristics of silicate-bearing inclusions in IAB iron meteorites examined in this work.

	Ni	Olivine	Ref.*	Low-Ca Px		Ref.*	High-Ca Px		Ref.*	Shock	Fe,Ni-Fes	$\Delta^{17}O$†	Inclusion
	(wt%)	Fa		Fs	Wo		Fs	Wo		stage	veins		type(s)‡
Caddo County	9.17	2.5–3.3	(1,10)	6.5	2.0	(1)	2.5–3	43.3–44.5	(1,10)	S2	yes	–0.42	ACS, NCS
Campo del Cielo	7.13	4.0	(2)	6.6	1.2	(2)	2.9	44.2	(2)	S2	no	–0.45	ACS
Copiapo	7.40	5.0	(2)	7.8	1.1	(2)	3.7	43.9	(2)	S2	no	–	ACS
EET 83333	8.06	5.0	(7)	7	–	(7)	–	–		–	–	–0.58	ACS
EET 84300	10.22	0.8	(7)	6	–	(7)	–	–		–	no	–0.50	ACS
EET 87504/5/6	–	3.0	(8)	6	–	(8)	–	–		S2	no	–	ACS
Four Corners	9.00	6.0	(2)	6.7	1.8	(2)	3.1	44.1	(2)	–	no	–0.38	ACS
Kendall County	5.5	–	–	1.0	0.7	(2)	0.8	44.8	(2)	–	–	–	ACS
Landes	6.58	4.0	(6, 9)	6.2	1.7	(6, 9)	3.2	45.6	(6)	S3	no	–0.44	ACS
Linwood	9.71	4.0	(2)	7.5	1.6	(2)	3.0	43.0	(2)	S2	no	–0.37	ACS
Lueders	6.92	4.5	(3)	6.6	1.5	(3)	3.0	44.7	(3)	S1	yes	–0.68	ACS
Mundrabilla	7.47	2.6	(5)	6.6	–	(5)	2.4	43.3	(5)	–	–	–0.46	SR
Ocotillo	7.09	3.4	(1)	5.8	1.5	(1)	2.8	44.4	(1)	S2	no	–0.67	ACS, NCS
Odessa	7.19	3.0	(2)	6.9	1.5	(2)	3.0	46.4	(2)	–	no	–0.30	RGR
Persimmon Creek	13.78	6.0	(2)	7.5	2.0	(2)	3.9	43.9	(2)	–	no	–0.50	SR, ACS
Pine River	8.32	1.0	(2)	4.0	1.2	(2)	1.9	44.3	(2)	S2	no	–0.52	ACS
Pitts	12.70	4.0	(2)	7.0	1.8	(2)	3.2	41.8	(2)	S2	–	–	SR
San Cristobal	24.97	3.1–3.3	(1, 4)	6.1–6.9	1.6	(1, 4)	–	–	–	–	yes	–0.56	PB
Tacubaya	7.86	6.0	(2)	6.9	1.2	(2)	2.7	44.5	(2)	–	no	–	ACS
TIL 91725	7.93	4.4	(1)	–	–		3.2	45.3	(1)	–	yes	–	ACS
Toluca	7.86	4.0	(2)	6.9	1.9	(2)	3.0	44.7	(2)	–	no	–0.49	RGR
Udei Station	9.71	8.0	(2)	8.7	1.7	(2)	3.5	42.3	(2)	S2-3	no	–0.48	NCS, ACS
Woodbine	9.70	6.0	(2)	7.9	2.1	(2)	3.5	43.9	(2)	S2	no	–0.46	SR, ACS
Zagora	9.70	4.8	(1)	6.7	1.7	(1)	2.9	45.4	(1)	–	–	–0.39	SR, ACS

Data on shock stage, presence of veins, and inclusion types from this work.
*References: (1) this work; (2) Bunch *et al.*, 1970; (3) McCoy *et al.*, 1996; (4) Scott and Bild, 1974; (5) Ramdohr *et al.*, 1975; (6) Bunch *et al.*, 1972; (7) *Antarctic Meteorite Newsletter* (1986); (8) *Antarctic Meteorite Newsletter* (1988); (9) Kracher, 1974; (10) Takeda *et al.*, 1993.
†Data on O-isotopic compositions from Clayton and Mayeda, (1996); Clayton and Mayeda, pers. comm. (1997).
‡Inclusion types: angular, chondritic silicates (ACS); nonchondritic silicates (NCS); sulfide-rich (SR); rounded, graphite-rich (RGR); phosphate-bearing (PB).

pyroxene (Fs_{1-9}), olivine (Fa_{1-8}), plagioclase (An_{11-21}), chromian diopside ($Fs_{2-4}Wo_{44}$), troilite, graphite, phosphates, and Fe,Ni metal and minor amounts of daubreelite and chromite (Table 3). Chromite is unusual in that it is rich in MgO and contains significant amounts of Al, V, and Zn in contrast with typical chondritic chromite compositions. Based on our examination of ~40 inclusions in 26 meteorites, the IAB iron meteorites contain a wide range of inclusion types, which are described most completely by the following categories: (1) sulfide-rich; (2) nonchondritic, silicate-rich; (3) angular, chondritic, silicate-rich; (4) rounded, often graphite-rich; and (5) phosphate-bearing inclusions (Table 3). Although the silicate minerals in these different inclusions are often similar in composition, the inclusions vary markedly in textures and modal mineral abundance. Here we describe the properties of each of these inclusion types, drawing upon observations and descriptions presented in the literature as well as our own observations.

Sulfide-Rich Inclusions

Sulfide-rich inclusions (labeled "SR" in Table 3 and Fig. 8) occur as irregular masses, rounded inclusions, or veins. We observed these in Mundrabilla (which has variously been classified as a IAB, IIICD iron, or both; Wasson *et al.*, 1980; Choi *et al.*, 1995), Pitts, Persimmon Creek, Zagora, Woodbine, and Toluca meteorites. These meteorites contain 7.2–13.8 wt% Ni in their metal and, thus, sample a significant portion of the total Ni range exhibited by silicate-bearing IAB iron meteorites. Sulfide-rich inclusions that we observed in Jenny's Creek and Canyon Diablo lack silicates and are not discussed further.

In Mundrabilla, sulfide-rich veins or lenses typically about a centimeter in width and 3–7 cm in length comprise about 25–35 vol% of the meteorite (Fig. 1) and generally occur along parent taenite grain boundaries (Buchwald, 1975). Each vein or lens generally consists of several centimeter-sized troilite grains. The inclusions often contain daubreelite and are sometimes partially rimmed by graphite, schreibersite, or both. Scott (1982) noted that the weak dendritic texture of the metal grains is a characteristic quench texture of metal-sulfide melts and suggested a cooling rate of ~5 °C/year during solidification. Rare angular silicate clasts ranging from a few millimeters to more than 1 cm are found within sulfide inclusions (Ramdohr *et al.*, 1975; Bild, 1977; Robinson and Bild, 1977; this work) throughout the 130 × 60 cm Mundrabilla slice (USNM 5730). The silicates are fine-grained (50–100 μm) and equigranular, similar in texture and mineral composition to some winonaite meteorites (*e.g.*, Mt. Morris (Wisconsin); Benedix *et al.*, 1998) and to silicate inclusions found in some other IAB iron meteorites (*e.g.*, Pine River). Opaque grains in these inclusions are commonly sulfides and only rarely metal.

Sulfide inclusions also occur as irregular (amoeboid, noncircular) masses in Pitts, Persimmon Creek, Woodbine (Buchwald, 1975), and Zagora meteorites. Woodbine and Zagora contain irregularly-shaped, sometimes vein-like, sulfide inclusions from a few millimeters up to 4 cm in length. The sulfide inclusions typically contain or border angular silicate clasts of a few millimeters in diameter, although the silicate clasts are not universally associated with sulfides. In Pitts and Persimmon Creek, the sulfide masses are more irregular but are also commonly

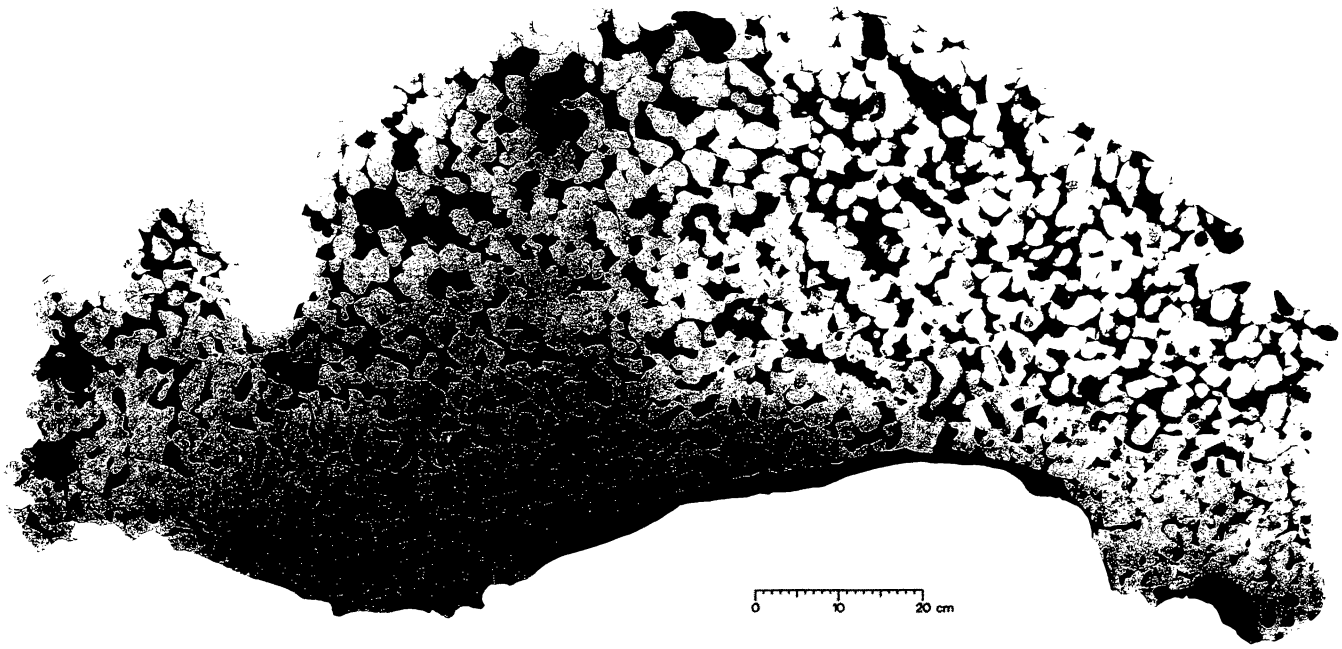

FIG. 1. Slab of the Mundrabilla iron meteorite showing metal-troilite intergrowths. This intergrowth texture is indicative of quenching from the liquidus implying that the molten metal was moved from within the parent body to a cooler region of the body within a short period of time to allow the quench texture to form. White areas are Fe,Ni metal and gray areas are troilite. Scale bar = 20 cm. (Photograph courtesy of P. Ramdohr *via* E. R. D. Scott.)

associated with angular silicate clasts. Rims of graphite, schreibersite, or both in contact with the troilite, common in Mundrabilla, were not apparent in hand samples of these meteorites.

A third morphology of sulfide inclusions can be found in several IAB iron meteorites, including Odessa and Toluca, which contain rounded (see Rounded, Often Graphite-Rich Inclusions below) sulfide-rich inclusions ranging from 1 to 6 cm in diameter. Silicates are rare in these meteorites, but we have observed angular silicate clasts contained in some sulfide-rich inclusions. In addition, graphite often occurs associated with these sulfide nodules; and schreibersite, cohenite, or both entirely rim the rounded inclusions.

Nonchondritic, Silicate-Rich Inclusions

Inclusions consisting of basaltic mineralogy are found in the Caddo County meteorite, whereas inclusions in Ocotillo containing coarse-grained olivine, plagioclase, and calcic pyroxene, may be basaltic to troctolitic in composition. These inclusions are labeled "NCS" in Table 3 and Fig. 8. Other types of nonchondritic inclusions are also found; for example, Campo del Cielo has veins of coarse-grained plagioclase and pyroxene with accompanying graphite (Wlotzka and Jarosewich, 1977). Olivine-rich inclusions found in the IAB iron meteorite Udei Station and some winonaite meteorites (*e.g.*, Winona, Mt. Morris (Wisconsin Range); Benedix *et al.* (1998)) also have nonchondritic mineralogy.

In hand sample, Caddo County displays abundant polymineralic silicate inclusions up to 7 cm in length (Fig. 2), some of which appear to be fragments of a much larger primary inclusion that was separated by metal veins. A striking feature of the hand sample is the presence of millimeter-sized, green chromian diopside crystals. These crystals tend to occur within the silicate clasts and do not constitute a separate inclusion type. The inclusion we studied in thin section is broadly basaltic in mineralogy, containing subequal proportions of coarse-grained plagioclase and mafic silicates (dominantly calcic pyroxene), with minor troilite and Fe,Ni metal. This specific inclusion has a coarse-grained (up to 3 mm grain size), gabbroic texture, similar to the many clasts studied and described in detail by Takeda *et al.* (1993, 1997, 2000). Takeda *et al.* (1993, 2000) reported that silicates inclusions containing fine-grained winona-like assemblages are also present and may be in physical contact with coarse-grained inclusions. Mafic silicates are relatively magnesian (olivine, $Fa_{2.5–3.3}$; low-Ca pyroxene, $Fs_{6.5}Wo_{2.0}$; calcic pyroxene, $Fs_{2.5–3}Wo_{43.3–44.5}$) and shock effects are minor (very weakly shocked, shock stage S2; Stöffler *et al.*, 1991). These mineral compositions are nearly identical to those reported from the roughly chondritic inclusions in the same meteorite (Palme *et al.*, 1991; Takeda *et al.*, 2000).

We studied four silicate inclusions in Ocotillo, each ~5 mm in diameter. Two of the inclusions are coarse-grained and dominated by plagioclase and olivine and by plagioclase and Cr-diopside (Fig. 3). Shock features in silicates are minor (unshocked to very weakly shocked, shock stages S1–S2; Stöffler *et al.*, 1991), and compositions of olivine ($Fa_{3.4}$), low-Ca pyroxene ($Fs_{5.8}Wo_{1.5}$), and chromian diopside ($Fs_{2.8}Wo_{44.4}$) are similar to those reported by Olsen and Schwade (1998) (Table 3).

We found a single centimeter-sized inclusion in Udei Station that is depleted in plagioclase (~3 vol%), compared with typical chondritic mineralogy (McSween *et al.*, 1991). Medium-grained (100–500 μm), equigranular olivine, low-Ca pyroxene and troilite, plus minor calcic pyroxene, chromite, and graphite are the dominant phases. This inclusion is best described compositionally as a peridotite and may represent the residue of partial melting. This clast contains the most Fe-rich mafic minerals found in the IAB iron meteorites, with olivine of $Fa_{8.0}$ and low-Ca pyroxene of $Fs_{8.7}Wo_{1.7}$.

Angular, Chondritic Silicate Inclusions

Many IAB iron meteorites contain angular silicate inclusions (labeled "ACS" in Table 3 and Fig. 8) that are roughly chondritic in mineralogy. These are different from the rounded, troilite-graphite-

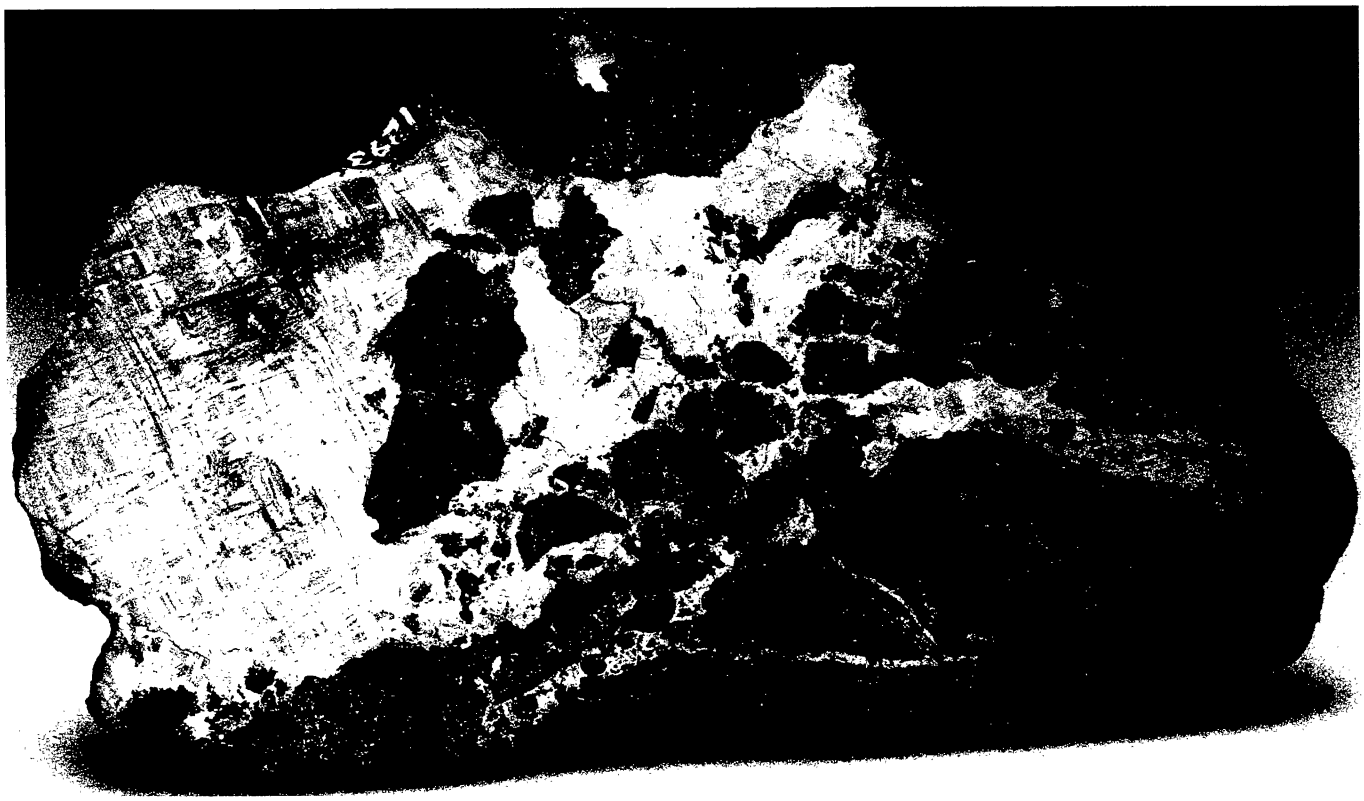

FIG. 2. Slab of Caddo County, showing truncated, polymineralic, and silicate-bearing inclusions up to 7 cm in size. Evidence for catastrophic impact is mainly in the coexistence of silicate inclusions and metallic matrix. These silicate-bearing inclusions comprise ~35 vol% of the slab. Maximum dimension of slab = 16 cm. (Photograph by Jeff Scovil.)

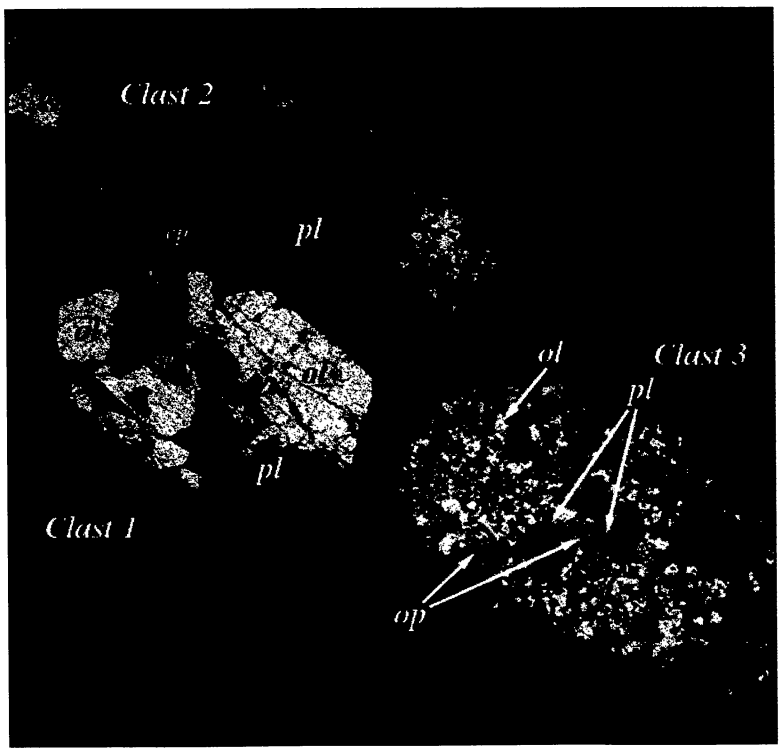

FIG. 3. Combined (merged) Mg and Al element map of Ocotillo, illustrating variation in types of clasts. Inclusions are shown *in situ* relative to one another. Clast 1 measures ~5 mm in maximum dimension and is composed primarily of plagioclase (pl) and olivine (ol), consistent with a troctolite composition. Clast 2 contains calcic pyroxene (cp) with plagioclase. The grain sizes of the minerals in this clast are less than those of the clast of basaltic composition in Caddo County. Clast 3 is a typical chondritic composition clast, similar to the angular inclusions found in many IAB iron meteorites, containing abundant orthopyroxene (op).

silicate-rich inclusions described in the next section. Angular silicate inclusions are found in Campo del Cielo (Wlotzka and Jarosewich, 1977; Bild, 1977; Fig. 4), Lueders (McCoy *et al.*, 1996), Copiapo, Pine River, Linwood, Four Corners, Pitts, Persimmon Creek (Bunch *et al.*, 1970), Elephant Moraine (EET) 83333, EET 84300, EET 87504/5/6 (*Antarctic Meteorite Newsletter*, 1986, 1988), Caddo County (Takeda *et al.*, 1993, 2000), Ocotillo (Olsen and Schwade, 1998), Thiel Mountains (TIL) 91725, and Zagora (Dominik and Bussy, 1994; this work). These meteorites have metal with a broad range of Ni contents (about 6.5–13.8 wt%). The metal phase in many of these meteorites is polycrystalline with the parent taenite grains ranging in size from millimeter- to centimeter-sized (Buchwald, 1975) These grains are small compared to the meter-sized parent taenite grains that are found in other IAB meteorites such as Canyon Diablo and Odessa. The abundance of inclusions varies from a few vol%, such as in the El Taco mass of Campo del Cielo, up to 40 vol% in Lueders, Landes, and Woodbine (*e.g.*, Mason, 1967; McCoy *et al.*, 1996). In some meteorites such as Lueders, adjacent silicate inclusions are separated by metal veins and have complementary borders, similar to the situation in Caddo County (Fig. 3), which suggests they were larger inclusions broken into fragments by intruding metal.

Silicates have three textural morphologies: fine-grained, recrystallized chondritic silicates; medium-grained silicates; and coarse-grained monomineralic crystals usually rounded and found individually in the metallic matrix, as first noted by Bunch *et al.* (1972). Major element analyses suggest that these silicate inclusions are similar in bulk composition to chondrites (Kracher, 1974; Bild, 1977). Measured rare earth element (REE) pattern shapes and abundances for Copiapo and Landes are essentially chondritic (Bild, 1977). The silicates are very weakly to weakly shocked (shock stages S2–3; Table 3). Inclusions of this type have the most FeO-poor silicate mineral compositions of any inclusions in the IAB iron meteorites. For example, Pine River has olivine of $Fa_{1.0}$ and Kendall County has pyroxene of $Fs_{1.0}Wo_{0.7}$.

Rounded, Often Graphite-Rich Inclusions

Several iron meteorites have rounded to ovoid inclusions (labeled "RGR" in Table 3 and Fig. 8) that contain variable amounts of silicate, graphite, and troilite, the latter two often being the dominant or sole constituents. Whereas the troilite-rich inclusions were discussed above, many of these meteorites contain mixtures of troilite, graphite, and troilite+graphite inclusions. We observed this type of inclusion in Odessa and Toluca and they occur in other IAB meteorites (*e.g.*, Canyon Diablo; Buchwald, 1975) not studied by us. These meteorites in general have a relatively narrow range of bulk Ni (6.8–7.9 wt%) in their metal and plot in the low-Ni cluster of IAB iron meteorites, although their metal chemistry is likely not related in any way to the presence or absence of this inclusion type.

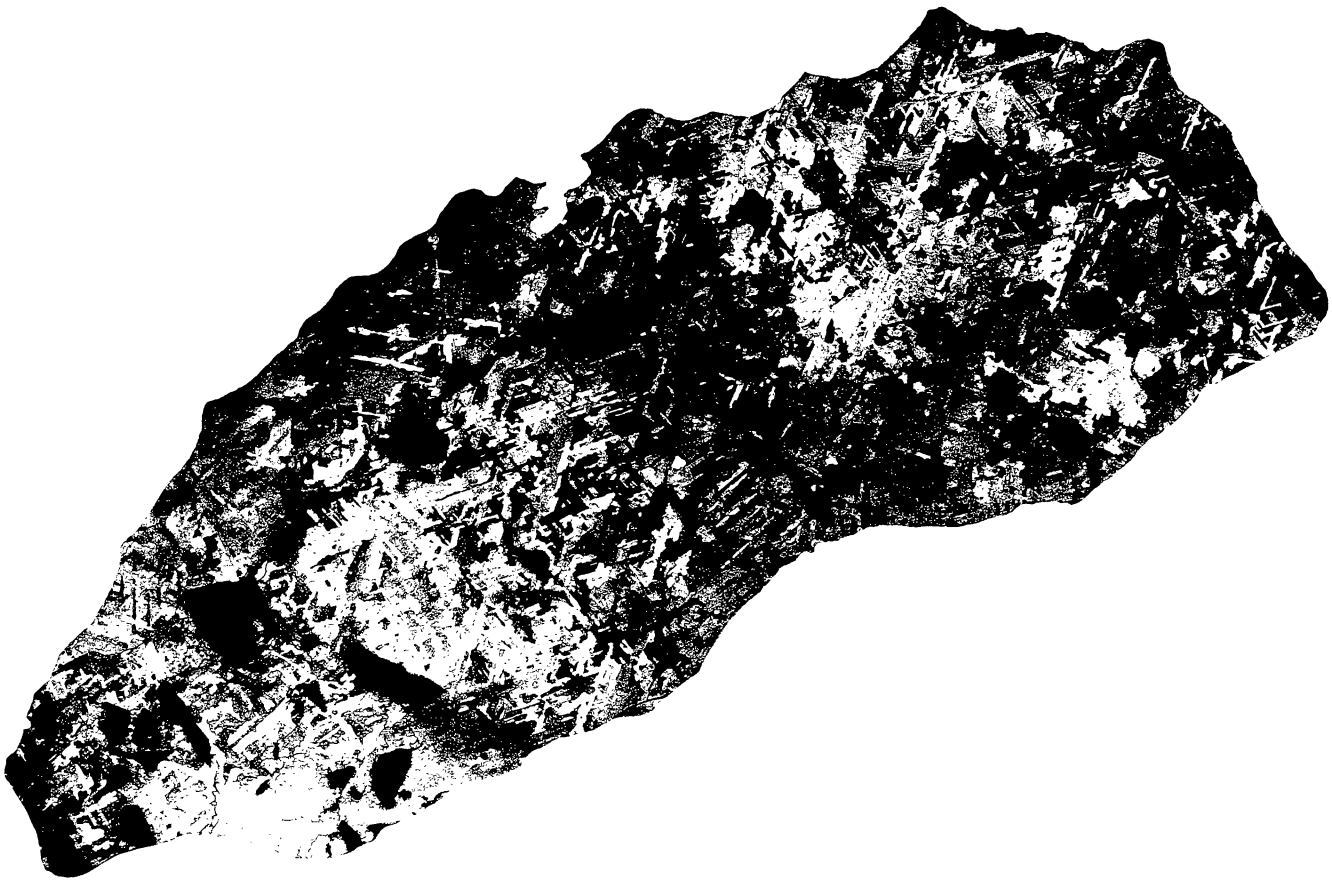

FIG. 4. Photograph of a large (~130 cm) polished slice of the Campo del Cielo IAB iron meteorite with common, heterogeneously distributed (both in size and spatial distributions) silicate inclusions. (Photograph courtesy of the Smithsonian Institution.)

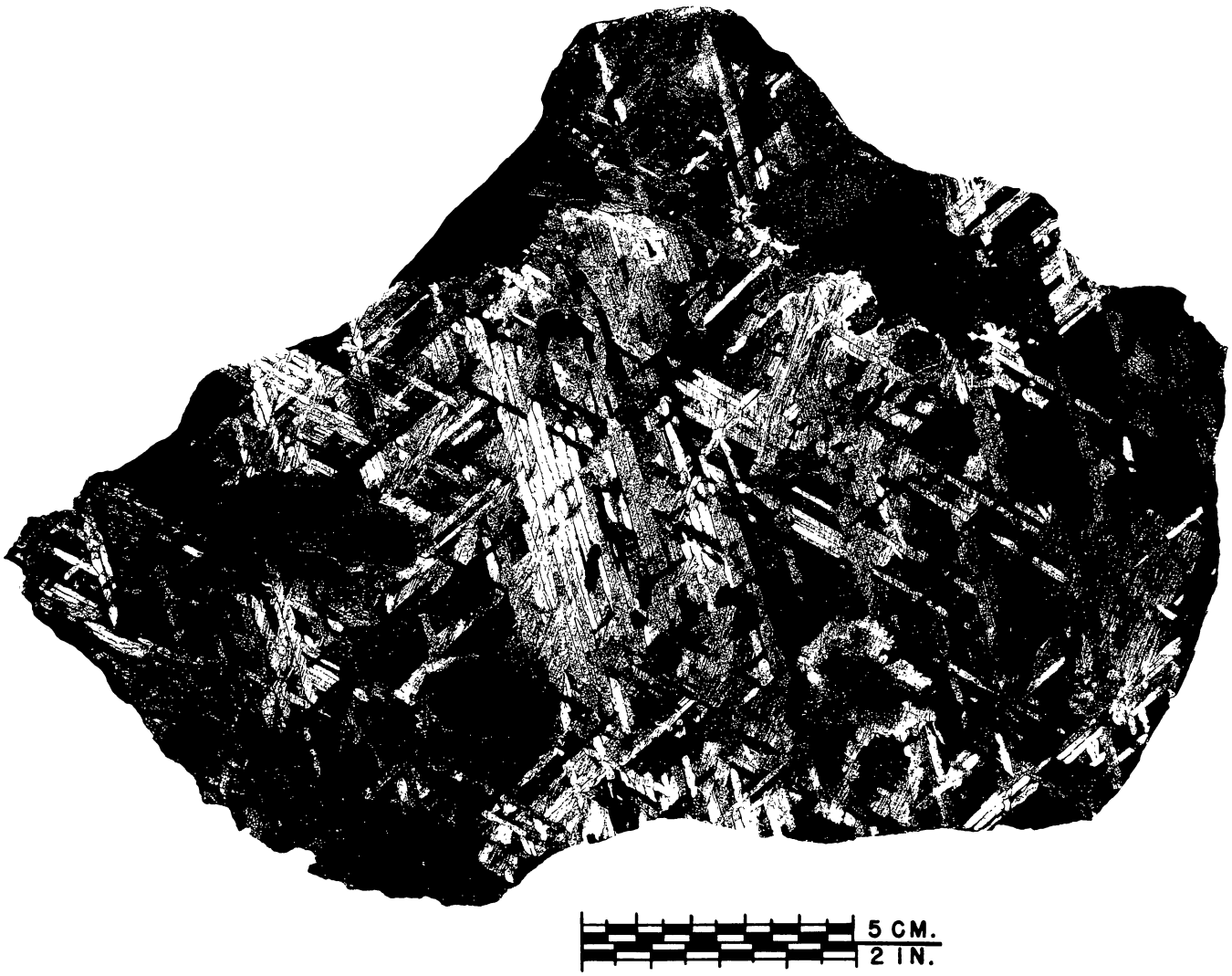

FIG. 5. Photograph of a cut and polished slice of the Toluca IAB meteorite (USNM no. 931) that contains the typical rounded graphite, and troilite-bearing, inclusions which sometimes contain angular silicate clasts (Photograph courtesy of the Smithsonian Institution.)

The cores of these inclusions consist of a combination of one or more silicates (although the presence of silicates is rare), troilite and graphite, often with a sequence of swathing minerals such as graphite, schreibersite, and cohenite. Inclusions that contain troilite and silicates are typically ovoid (egg-shaped), whereas the graphite-troilite-rich inclusions tend to be more circular. The silicate cores, when present, are angular, generally surrounded by centimeter-sized troilite areas, and always occur with either troilite or graphite-troilite surrounding them. We have observed these inclusion types in Toluca (Fig. 5). Marshall and Keil (1965) and Buchwald (1975) reported similar characteristics for inclusions in Odessa and Canyon Diablo. Mafic silicates are Fe-poor (Fa_{3-6}; Table 3) and are similar in composition to those of silicates in other IAB iron meteorites. In addition to the mafic silicates, several atypical phases, such as the Na-Cr-rich pyroxene kosmochlor (*e.g.*, Olsen and Fuchs, 1968), are also found in rounded, graphite-rich inclusions.

Phosphate-Bearing Inclusions

Phosphates are found in trace amounts in many IAB iron meteorites. The most common phosphate is chlorapatite or whitlockite (Bunch *et al.*, 1970). However, San Cristobal (24.97 wt% Ni; Choi *et al.*, 1995), described by Scott and Bild (1974), is unusual in containing the Mg-Na-bearing phosphate brianite in moderate abundance. Interestingly, Fuchs (1969) also reported brianite in the low-Ni IAB Youndegin (6.80 wt% Ni), although neither compositional data nor the source of the section in which this mineral occurred was given. Phosphate-bearing inclusions are labeled "PB" in Table 3 and Fig. 8.

The one silicate inclusion we examined in the thick section of San Cristobal is subangular in shape and incompletely rimmed by schreibersite. Veins of troilite and Fe,Ni metal cross-cut the inclusion. The silicates are equigranular and appear to be recrystallized, and plagioclase comprises ~12% of the total silicates. Silicate compositions (olivine, $Fa_{3.1-3.3}$; low-Ca pyroxene, $Fs_{6.1-6.9}Wo_{1.6}$; Table 3) are within the range of those of other silicate-bearing IAB iron meteorites. A trace amount of graphite rims the inclusion and cohenite is observed in the metallic host. Brianite, identified in San Cristobal by Bild (1974), comprises 3.7 vol% of the silicate inclusion (Fig. 6) and is scattered throughout the silicates but tends to be in contact with metal, either as veins within the silicates or at the edges of the inclusion.

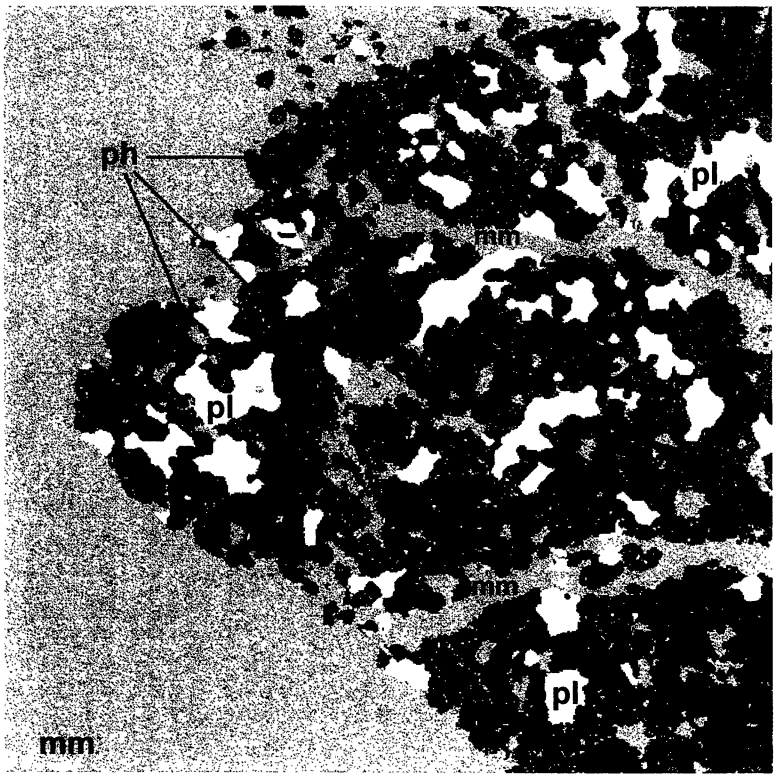

FIG. 6. Merged Mg + Al element map illustrating the distribution of phosphates in a silicate inclusion in San Cristobal. The phosphate brianite ($Na_2CaMg(PO_4)_2$) (ph; dark gray) comprises 3.5 vol% of the inclusion which is dominated by low-Ca pyroxene (op; dark medium gray) with lesser amounts of olivine (ol; light medium gray) and plagioclase (pl; light gray). The clast is embedded in the metallic matrix (mm). The field of view of the figure is ~5 mm.

DISCUSSION

The data presented here, in combination with the results of previous work, constrain the geologic history of the IAB iron meteorite parent body. Here we discuss whether IAB and IIICD iron and the stony winonaite meteorites originated on a common parent body. We also briefly review previous models and present our hypothesis for the origin of these meteorites.

A Common Parent Body for IAB and IIICD Iron and Winonaite Meteorites?

It is highly likely that the stony winonaite meteorites and the IAB iron meteorites are from the same parent body. Essentially identical O-isotopic compositions (Clayton and Mayeda, 1996) imply a common O-isotopic reservoir and are consistent with an origin on a common parent body. Mineralogies and mineral compositions of silicates overlap between winonaites and silicate inclusions in IAB iron meteorites (Bild, 1977; Benedix *et al.*, 1998; this work). The textures of some silicate inclusions in some IAB iron meteorites, particularly the angular, chondritic clasts, are nearly identical to the textures of winonaites (Fig. 7). It should be noted that certain textures seen in silicate inclusions of IAB iron meteorites (*e.g.*, basaltic and troctolitic textures in Caddo County and Ocotillo) are not observed in the winonaites, and some textures of winonaites (*e.g.*, the chondritic Pontlyfni and the coarse-grained granoblastic texture in Tierra Blanca; Benedix *et al.*, 1998, and references therein) are not observed among the inclusions in IAB iron meteorites. Thus, in the likelihood that winonaite and IAB meteorites are indeed from the same parent body, both groups taken together provide a more complete sampling of the diversity of rock types observed on their common parent body than does either group alone. Cosmic-ray exposure ages, commonly used to indicate sampling of meteorites by a common cratering event on a single parent body, are considerably different for winonaites (0.02–0.08 Ga; Benedix *et al.*, 1998) and IAB iron meteorites (0.4–1.0 Ga; Voshage, 1967). These ages can only be used to infer that the meteorites were liberated from the parent body in different events.

Less certain is whether IAB iron–winonaite meteorites and IIICD iron meteorites sample a common parent body. Some properties of these rocks are clearly consistent with such an origin. Oxygen-isotopic compositions of silicates from inclusions in IAB and IIICD iron and winonaite meteorites are essentially indistinguishable (Clayton and Mayeda, 1996). Choi *et al.* (1995) suggested that the IAB and IIICD meteorites sample a common parent body based on trends in the trace element compositions of the metal of these two meteorite groups. In addition, inclusions broadly similar in mineralogy to those in IIICD iron meteorites are found among the IAB iron–winonaite meteorites (McCoy *et al.*, 1993; Benedix *et al.*, 1998; this work). However, important differences exist in mineral compositions: Pyroxene compositions of inclusions in IIICD meteorites extend to higher Fs contents and plagioclase compositions are consistently more albitic than those in IAB iron–winonaite meteorites (McCoy *et al.*, 1993). Thus, whereas the link between IAB iron and winonaite meteorites appears robust, several lines of evidence exist to question a strong link between these groups and IIICD iron meteorites. Further recoveries of additional meteorites will be necessary to establish whether these apparent differences are simply sampling biases.

Previous Hypotheses for the Formation of IAB Iron and Winonaite Meteorites

Although few hypotheses have been postulated for the formation of the winonaites, several have been suggested for the IAB iron meteorites. Wasson (1972) argued that elemental trends in IAB iron meteorites were due to condensation directly from the nebula, giving rise to the term "non-magmatic". However, this hypothesis was later rejected by Wasson *et al.* (1980) because, if the variations in elemental abundances are due to nebular processes, comparable ranges in the metal compositions should be found in chondritic material as well, which is not the case. Another problem with this hypothesis is the difficulty of forming, by condensation, parent taenite crystals tens of centimeters in size (Wasson *et al.*, 1980).

Wasson *et al.* (1980) and Choi *et al.* (1995) suggested that the IAB iron meteorites formed in numerous localized impact-melt pools in the chondritic megaregolith of their parent asteroid. They argue that impacts would selectively melt metal and sulfide that would migrate to form pools. Impacts are thought to have occurred over a range of time and temperatures, producing the correlated variations between Ni and Ga, Ge, and Ir. In an extreme view, each IAB iron meteorite represents an individual melt pool. Although the pools would cool relatively quickly, trapping the unmelted, angular silicate inclusions, Choi *et al.* (1995) argued that both limited fractional crystallization and magma mixing occurred to

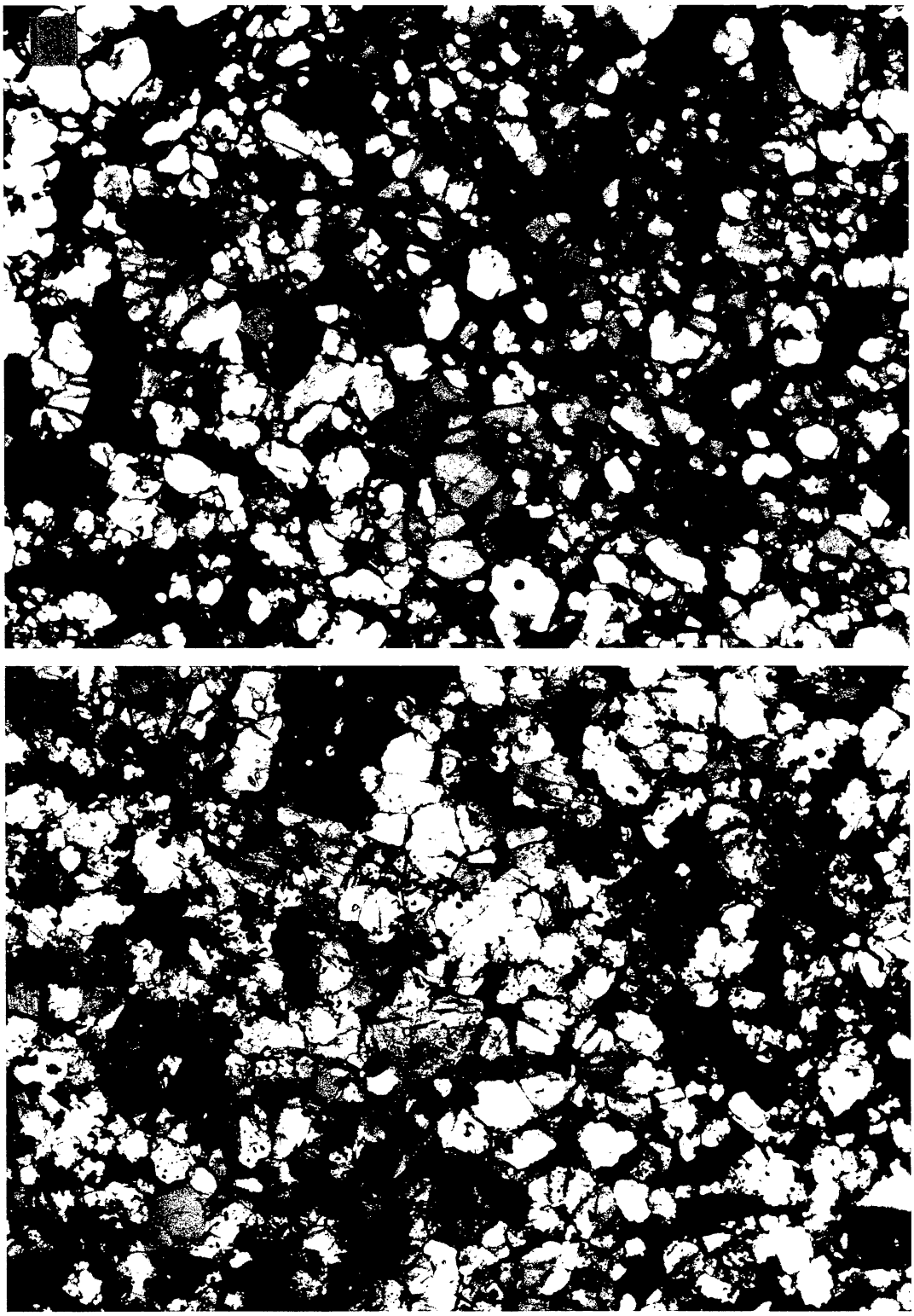

FIG. 7. Photomicrographs showing similarity in texture of silicates between IAB iron and winonaite meteorites. (a) Recrystallized, medium-grained Winona (USNM 854-1). Field of view is 2.6 mm. (b) Texture of a silicate inclusion in Campo del Cielo (from the El Taco mass; USNM 5615). Field of view is 2.6 mm.

produce the high-Ni IAB iron meteorites and the scatter in Ga, Ge, and Ir observed at high-Ni concentrations. Although impact does provide a ready mechanism for mixing silicates and metal, the main problem is that impacts seem incapable of producing copious quantities of Fe,Ni-FeS-rich melts. Keil *et al.* (1997) argue, based on theoretical, experimental and observational evidence, that selective melting by impact occurs only locally and produces an extremely low percentage of melt. Any melt produced quenches rapidly, thus inhibiting fractional crystallization and migration of selective melts into larger pools, as is required for the formation of the largest IAB iron meteorites.

Several authors have proposed that IAB and IIICD iron meteorites formed as a result of partial melting and core formation on a differentiated asteroid. Kelly and Larimer (1977) argued that the composition of the metal is consistent with fractional melting of a single composition that was isolated from later melted material so that it would not reequilibrate. Wasson *et al.* (1980) marshaled several arguments against this model, the most compelling of which is the apparent contradiction between predicted and measured siderophile element partition coefficients and the unreasonably high temperatures required to form the last fractional melts. Kracher (1982, 1985) showed that IAB and IIICD trace element trends could be explained by fractional crystallization of a metallic melt formed during partial melting of a S-rich parent body. Using this model to illustrate the general features of trace element behavior, he suggested that migration of the Fe,Ni-FeS eutectic melt could result in the formation of a S-rich core at low temperatures. However, Choi *et al.* (1995) argued that crystallization of such a magma cannot produce the observed distribution of Ni concentrations. In addition, both McCoy *et al.* (1993) and Choi *et al.* (1995) recognized that the presence of any significant C or P in the melt could complicate the system even further. McCoy *et al.* (1993) argued that correlated trends between the properties of IIICD silicate-bearing inclusions (*e.g.*, mineral compositions and modal mineralogies) and the Ni concentrations of the metallic host are best explained by reaction between silicates and metal during a prolonged period of fractional crystallization of a common metallic magma. Finally, Takeda *et al.* (1994, 2000) suggested that partial melting of the parent body was accomplished by a combination of ^{26}Al decay and small-scale impacts of high-speed projectiles on the surface. Most of the supporting evidence for this model was taken from a study of the lodranites. Whereas the acapulcoite-lodranite meteorites are also primitive achondrites, they are clearly not from the same body as the IAB meteorites, as evidenced by their O-isotopic compositions.

A serious flaw of any of the partial melting models is the inability to readily account for the mixing of unmelted silicate clasts into a liquid metallic Fe,Ni core. This is particularly problematic in an asteroidal core, which probably crystallized from the outside, thus armoring the inner core (Choi *et al.*, 1995). Kracher (1982, 1985) argued that silicates may have been spalled into the core from the core–mantle boundary by impact-generated tectonic activity, but no supporting modeling has been done that could suggest how this mechanism would actually work. Takeda *et al.* (1994, 2000) argued silicates and metal were mixed by melt migration. This could take place over a prolonged heating time because of density differences (Marangoni convection; Takeda *et al.*, 2000), but determinations of the various radiometric ages indicate that much of the geology occurred on the parent body very early and quickly in the history of the solar system. No data were given on the amount of time required for this method of melt migration to occur.

We present a hypothesis for the formation of the IAB meteorites that combines both partial melting and impact processes to account for the various compositional and textural features found in these meteorites. This is, in some ways, a detailed extension of the model presented by Takeda *et al.* (1994) that partial melting and impact combined to produce the IAB meteorites. The main difference being that, for reasons presented above, impact was not a heat source for the partial melting.

Hypothesis for the Formation of IAB Iron and Winonaite Meteorites

We propose the following scenario for the origin of the IAB iron and winonaite meteorites: (1) A chondritic parent body was heated by a noncollisional heat source. (2) It experienced partial melting, incomplete separation of melt from residue and metamorphism, possibly creating a number of molten metal bodies throughout the parent body. (3) A catastrophic impact caused fragmentation, followed by gravitational reassembly of the parent body. (4) Reassembly caused extensive mixing of silicates, metal, and sulfide. (5) Molten metal bodies on the reassembled body fractionally crystallized. This entire process occurred very early in solar system history. Figure 8 schematically illustrates this model, which we discuss in detail below.

Precursor Material–The bulk compositions and mineralogies of winonaites and silicate inclusions in IAB iron meteorites (*e.g.*, Jarosewich, 1967; Kracher, 1974; Benedix *et al.*, 1998) resemble those of chondritic meteorites. The chondritic nature of the precursor material is also strongly supported by the presence of highly recrystallized relic chondrules in the winonaite Pontlyfni (Benedix *et al.*, 1998, and references therein). However, O-isotopic compositions of the silicate inclusions in IAB iron meteorites and of the winonaites are unlike those of any existing chondrite group (Clayton and Mayeda, 1996). Further evidence for this is the unusual composition of chromite in these meteorites, implying that the starting composition was slightly different than that of known chondrites. These lines of evidence suggest that the pristine chondritic precursor material of the IAB iron and winonaite meteorites is not represented in the world's meteorite collections.

Heating and Partial Melting–Studies of IAB iron and winonaite meteorites (this study; Takeda *et al.*, 1994, 2000; Benedix *et al.*, 1998) suggest that their parent body experienced heating and partial melting. The presence of relic chondrules in the winonaite Pontlyfni and the recrystallized textures of silicates in winonaites and IAB iron meteorites indicate metamorphic temperatures at least as high as those experienced by petrologic type-6 ordinary chondrites (about 750–950 °C; Dodd, 1981).

Several lines of evidence suggest that temperatures in parts of the IAB–winonaite parent body were sufficient for partial melting. Two-pyroxene geothermometry yields temperatures up to 1200 °C (*e.g.*, Tierra Blanca; Benedix *et al.*, 1998). At these temperatures, both Fe,Ni-FeS cotectic melting, which occurs at ~950 °C (Kullerud, 1963; Kubaschewski, 1982), and silicate partial melting to produce basaltic melts, which occurs at ~1050 °C (Morse, 1980), are possible. Veins of Fe,Ni metal and troilite in winonaites (*e.g.*, Pontlyfni, Winona; Benedix *et al.*, 1998) may represent cotectic melts. The metallic matrix of most IAB meteorites and the presence of metal-sulfide-rich IAB meteorites (*e.g.*, Zagora, Pitts) is further evidence that Fe,Ni-FeS partial melting must have occurred on this

TABLE 4. Model initial conditions and final scrambled core percentages for impacts at 5 km/s with an impact angle of 45°.

		Undifferentiated		Differentiated	
Target diameter (km)	Projectile diameter (km)	% Target material retained	% Original core scrambled	% Target material retained	% Original core scrambled
100	15.8	70	24	78	9
300–316	78.8–79	72	22	71	7

parent body and that these melts migrated and pooled. There is further evidence that this temperature was exceeded in portions of the parent body. A liquidus temperature of ~1390 °C is inferred for the sulfide-rich Mundrabilla iron meteorite (Scott, 1982). Based on the variations in Ni content of the metal as well as textural features, it is difficult to determine whether there was a single, S-rich core or several smaller melt bodies scattered throughout the body. The existence of several very large IAB iron meteorites (*e.g.*, Canyon Diablo) requires that some melt bodies must have been many tens of meters in diameter.

Peak temperatures in the IAB–winonaite parent body of 1200–1400 °C, as discussed above, produced silicate partial melting. These temperatures also indicate that the body may have begun to differentiate. Crystallized silicate partial melts are observed in both winonaite and IAB iron meteorites. Trapped basaltic partial melts are sampled as both fine-grained calcic pyroxene-plagioclase-rich areas in Pontlyfni (Benedix *et al.*, 1998) and coarse-grained, gabbroic clasts in Caddo County (Takeda *et al.*, 1994, 1997, 2000; this work) and, possibly, Ocotillo (this work). Partial melting and melt removal has been suggested to explain variations in pyroxene and plagioclase abundances between silicate inclusions in Campo del Cielo (Wlotzka and Jarosewich, 1977; Takeda *et al.*, 2000). Complementary depleted residues are also present in these meteorites. Olivine-rich regions in Winona and Mt. Morris (Wisconsin) (Benedix *et al.*, 1998) and olivine-orthopyroxene-rich clasts in Udei Station (this work), both of which are virtually devoid of plagioclase, may represent residues formed by removal of a basaltic melt fraction and may have required temperatures of up to 1250 °C (Taylor *et al.*, 1993). Oxidation-reduction may have also occurred during partial melting. For example, oxidation of daubreelite commonly found in primitive winonaites might explain the formation of chromian diopside found in some winonaite and IAB iron meteorites. In addition, this process may also account for the presence of the rare Cr-rich phases krinovite and kosmochlor found in the rounded graphite-rich inclusions (as described above). However, the occurrence of these oxidized phases in the presence of graphite nodules is difficult to explain and detailed thermodynamic calculations need to be carried out to address this problem.

The inefficiency of impact as a global heat source (Keil *et al.*, 1997) suggests that heating of the chondritic precursor body of the IAB iron–winonaite meteorites was noncollisional and, most likely, the result of the decay of short-lived ^{26}Al (MacPherson *et al.*, 1995). Substantial thermal gradients must have existed in this body, as peak temperatures for different winonaite and IAB iron meteorites vary by as much as ~400 °C. Thermal gradients of this magnitude are not uncommon for meteorite parent bodies (Dodd, 1981) and asteroid thermal models predict such gradients (Ghosh and McSween, 1998). Because of this, we cannot rule out that some melt bodies partially or wholly crystallized prior to the impact.

Collisional Fragmentation and Gravitational Reassembly–A major puzzle in explaining the origin of IAB iron meteorites is the mechanism that mixed molten metallic Fe,Ni-FeS with solid silicate rock fragments. Based on theoretical studies of the collisional evolution of asteroids (*e.g.*, Davis *et al.*, 1979; Hartmann, 1979; Melosh and Ryan, 1997) and on evidence from the study of meteorites (*e.g.*, Taylor *et al.*, 1987; Keil *et al.*, 1994), it has been suggested that major impacts can fragment asteroids without causing permanent dispersal of all of the debris. In these scenarios, gravitational reassembly may take place to form bodies that are "rubble piles" of material from diverse depths in the original body. We now present results of computer simulations that test the feasibility of mixing of differing lithologies from various depths in a partially differentiated asteroidal-sized body.

Although we are uncertain if the IAB–winonaite parent body had a single fully developed core or several sizable molten metal pockets distributed throughout the body prior to impact, we have explored the efficiency of impact scrambling of a differentiated body. Love and Ahrens (1996) applied numerical hydrodynamic simulations of impacts to homogeneous, gravity-dominated asteroids and we have applied this same model to differentiated asteroids. This procedure employs a three-dimensional smoothed particle hydrodynamics (SPH) code that models a continuous medium using discrete particles whose physical properties are mathematically "smoothed" out into the neighboring volume. It is good for simulating hypervelocity impacts, because it remains accurate even when the collision partners suffer extreme geometrical distortion (*e.g.*, Monaghan, 1992). It is found that after the hydrodynamic phase, some of the target asteroid's mass carried enough kinetic energy to climb at least to the surface if launched from the target's center, or to enter orbit around the target if launched from the surface, but did not possess enough energy to escape. This displaced mass, which is transported from its original depth, is called "scrambled" and could re-accrete anywhere on the final rubble pile. Love and Ahrens (1996) found that a significant fraction of the final target can be scrambled, but only in impacts that also permanently eject much of the target's mass. For example, in order to get 50% of the final rubble pile (equivalent to ~25% of the original mass) to be relocated from its original location (*i.e.*, scrambled), half of the original target mass is destroyed. They also calculated the percentage of the final rubble pile consisting of scrambled particles excavated from the deep interior ("core") of the (homogeneous) rocky target. "Core" material was identified as that initially lying within half the target's initial radius of the target center. Only the largest impacts scrambled significant mass (up to ~10 % of the final body's mass) from the "core".

Extending those results to differentiated targets must be done cautiously. A dense Fe,Ni core in a differentiated asteroid is bound to itself more tightly by gravity than a "core" of the same size made of stony material. This extra binding, working together with the drop in shock velocity that accompanies a transition from a low density to a high density medium, hinders excavation of core material. The "core" scrambling results of Love and Ahrens (1996)

using uniform granite targets thus provide only an upper limit on the effectiveness of that process in differentiated targets. With this caveat in mind, we have extended this work to treat asteroids 100 and 300 km in diameter with Fe cores occupying the central 9% of their volumes. This fraction represents the amount of metallic Fe,Ni-FeS obtained by complete removal of the metal and troilite fractions of an H-chondrite starting composition into a core and, thus, is an extreme case of a fully differentiated parent body. An impact velocity of 5 km/s (the mean collision speed for asteroids with each other) and impact angle of 45° (most likely impact angle) was used for all trials with differentiated bodies, and Table 4 shows the results for undifferentiated and differentiated targets. As expected, impacts into differentiated or undifferentiated targets have little effect on the amount of target permanently lost from the body (particularly at larger sizes). However, for identical impacts, scrambling of core material is less effective in differentiated targets than in homogeneous ones. This is partly due to the extra gravitational "strength" a differentiated asteroid gains from its dense core, allowing it to endure somewhat larger impacts. These effects combine such that catastrophic impacts (those permanently removing about half the target mass) on large differentiated asteroids yield final rubble piles containing about 5–10 vol% of material excavated from the core. Thus, mixing of material from the center of the body is less effective for differentiated than for undifferentiated asteroids. Nonetheless, these calculations suggest that catastrophic fragmentation and gravitational reassembly as a mechanism for mixing metal and silicates in a totally differentiated asteroid is possible. Thus, it seems likely that in the case of a partially differentiated asteroid such as the IAB iron–winonaite precursor body, the magnitude of scrambling would be greater than in the calculated extreme case of a completely differentiated object. It should be noted that the dominance of IAB iron meteorites over winonaites in the world's collections has no relevance to the question of the original amount of core material (about 5–10 vol%) that was scrambled. These meteorites were produced by more recent impacts, including collisions in space. It is well known that the half-lives of iron meteoroids in space are much greater (by a factor of >50) than those of stone meteoroids (*e.g.*, Caffee *et al.*, 1988) and this is consistent with the longer cosmic-ray exposure ages of the IAB meteorites compared to winonaites. Thus, it is not surprising that from a totally shattered, differentiated asteroid, iron meteorites would be more abundant than stones.

Mixing of Metal, Sulfides, and Silicates During Reassembly– Using the results of the SPH code as general guidelines for the feasibility of such a scenario, we suggest that the partially melted and incompletely differentiated IAB iron–winonaite parent body experienced catastrophic breakup and reassembly while near its peak temperature. This is because we cannot think of another process that could mix molten core (metal-troilite) and solid surface (silicate) materials on an asteroidal scale and then bury some of the mixtures sufficiently deeply so that Widmanstatten structures formed in the metal during subsequent slow cooling below ~700 K. We assume that the mixing occurred in a single fragmentation event because we see no evidence of multiple mixing events, such as pre-existing metal-silicate structures in the metal, like those seen in the mesosiderites (*e.g.*, Cowan and McCoy, 1998). Resulting fragmentation of the body and gravitational reassembly of some of the debris caused "scrambling" and mixing of the various lithologies and melts (Fig. 8).

At the time of the catastrophic breakup of the IAB–winonaite precursor body, partial melting and metamorphism appears to have produced five lithologies consisting of:

- Metallic melts (where temperature (T) could have been as high as ~1400 °C);
- sulfide-rich, metallic melt (found in regions where T was at least 950 °C);
- Metamorphosed, chondritic silicates (where the maximum T was ~950 °C);
- Molten and crystallized silicate partial melts (where the minimum T was ~1050 °C);
- Silicate-rich residues of partial melting (where the T could have reached up to ~1250 °C).

During reassembly, following the impact, these five basic lithologies and melts were mixed (denoted by jagged ovals in Fig. 8) in various combinations. However, we see some lithologies in the IAB iron and winonaite meteorites that do not appear to have experienced mixing during the fragmentation event. These include:

- Inclusion-free metallic melts (labeled "M" in Fig. 8). These crystallized before or after the impact event and include meteorites formed by extensive fractional crystallization in large melt bodies.
- Metamorphosed, chondritic silicates. These silicates, which are represented by some winonaites, experienced only metamorphism on a centimeter scale and do not contain evidence of mixing with more metamorphosed or molten metal lithologies (*e.g.*, Queen Alexandra Range (QUE) 94535 and Tierra Blanca).

The following lithologies are found in IAB iron and winonaite meteorites and are best explained as having formed as the result of mixing due to impact:

- Angular chondritic silicates. These lithologies formed by mixing abundant, angular fragments of cooler, metamorphosed, chondritic silicates into metallic melt, causing rapid cooling and solidification (Onorato *et al.*, 1978) of the molten metal (*i.e.*, small parent taenite grains), thus preventing density fractionation (*e.g.*, Landes, Lueders, Campo del Cielo, and Pine River, among others).
- Non-chondritic silicates. Clasts of residue material (labeled "R" in Fig.8) or fragments of crystallized partial melts (labeled "pm" in Fig. 8) were mixed with molten metal to form this type of lithology (*e.g.*, Udei Station and Caddo County).
- Sulfide-rich, silicate-rich inclusions. Abundant, angular silicates that were mixed into sulfide-rich metallic melts (*e.g.*, Pitts, Persimmon Creek, Woodbine, and Zagora).
- Sulfide-rich, silicate-poor inclusions. Some S-saturated, metallic melt bodies quenched during the impact event, inhibiting, but not prohibiting, the trapping of silicates within the metallic matrix. An example is Mundrabilla, which contains abundant sulfide and minor silicates. Fast cooling at the time of solidification, possibly a result of this mixing, is indicated for Mundrabilla, with a cooling rate of ~5 °C/year (10^{-7} °C/s) (Scott, 1982).
- Silicate-silicate inclusions. Silicates mixed together in the near-absence of the metal-sulfide-rich melts and contain mixtures of residues and metamorphosed chondritic silicates. Also, mixtures of coarse- and fine-grained silicate textures that could not have formed together (*e.g.*, Winona, Mt. Morris (Wisconsin), and Yamato 75300; Benedix *et al.*, 1998).

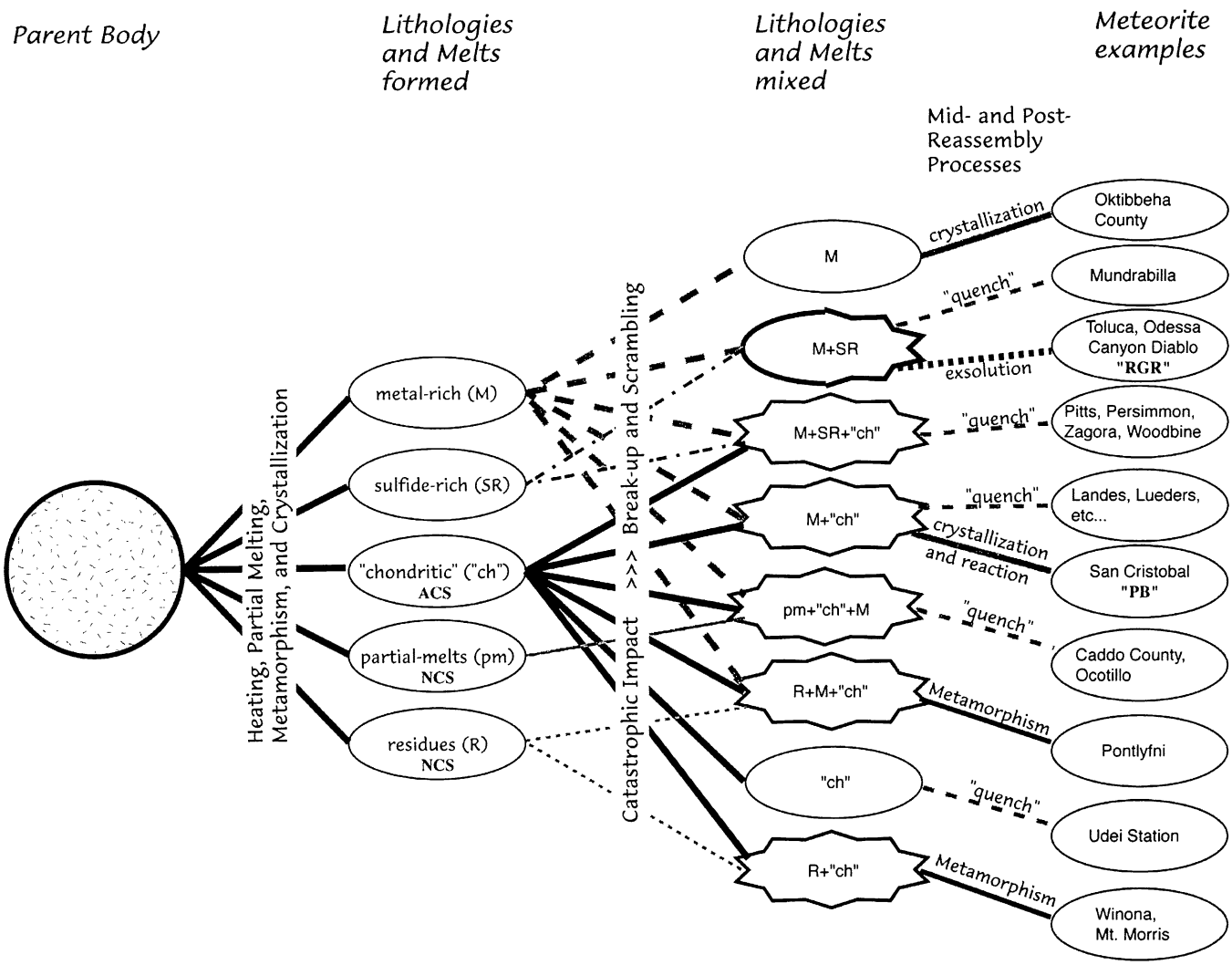

FIG. 8. Flow chart illustrating the model presented here for the origin and formation of the winonaite and IAB iron meteorites. Circles and ovals represent lithology types and lines link lithologies *via* various processes (which may be denoted on the line). Lithologies and melts in the flow chart are correlated with the various inclusion types described in the text. The chondritic parent body was heated, partially melted, and metamorphosed and produced the five lithologies and melts prior to breakup as indicated in the first set of ovals. These are metal-rich (M) and sulfide-rich lithologies/melts (SR), chondritic ("ch") lithologies, and partial melts (pm) and residues (R). After breakup and reassembly, at least eight lithologies/melts formed in the reassembled rubble-pile body (second set of ovals; the jagged outlines indicate that mixing of lithologies/melts took place during the breakup and reassembly event; the half-smooth and half-jagged oval for M + SR denotes that some M + SR inclusions were formed by exsolution from the metal-rich melt and other M + SR inclusions were formed because of mixing with silicate clasts or quenching of the metal melt). The last set of ovals lists some meteorite examples of the different lithologies. The lines connecting the second and third sets of ovals denote the physical processes that were involved in the formation of the specific meteorites listed. (RGR = rounded, graphite inclusions, PB = phosphate-bearing, NCS = nonchondritic silicate-rich inclusions, and ACS = angular, chondritic silicate inclusions).

Fractional Crystallization, Metamorphism, and Cooling– After reassembly of the body, enough heat was retained because of the opacity of the dust cloud created by the impact that large molten metal bodies continued to evolve through fractional crystallization, reaction with entrained silicates, and liquid immiscibility (Scott, 1972; Kracher, 1982, 1985; Choi *et al.*, 1995). It appears that some metallic melt bodies either remained intact or were not thoroughly mixed with silicate material during parent-body breakup and reassembly. This is indicated by the occurrence of rounded, graphite-troilite-rich, silicate-poor inclusions found in Toluca, Odessa, and Canyon Diablo that almost certainly formed by exsolution from the still molten metal (Buchwald, 1975). High-Ni IAB iron meteorites such as San Cristobal (25 wt% Ni) and Oktibbeha County (60 wt% Ni) formed by fractional crystallization in metallic bodies that cooled slowly over long time periods (Scott, 1972; Kracher, 1982, 1985; Choi *et al.*, 1995). Reaction of metallic melts with entrained silicate clasts probably produced the evolved, Na-Mg-phosphates found in San Cristobal, analogous to the process that formed similar phosphates in IIICD iron meteorites (McCoy *et al.*, 1993). Phosphates also could have formed during solidification of the metal that would have concentrated P and O in the residual liquid (Olsen *et al.*, 1999). Slow cooling of the reassembled parent body resulted in complete solidification. Zoning in both metal grains in the silicate inclusions and in the taenite lamellae of the metallic host of IAB iron meteorites suggests cooling rates of 25 to ~200 °C/Ma (Herpfer *et al.*, 1994). Reduction of silicates is a

ubiquitous feature of IAB iron meteorites, producing olivines with Fa less than Fs in coexisting low-Ca pyroxene (Table 3 and references therein). Such reduction is not unexpected, given the prolonged cooling history of these C-rich rocks. The relatively old ages of silicate inclusions in IAB iron meteorites of 4.43–4.53 Ga (Bogard *et al.*, 1968, 1999; Niemeyer, 1979a,b; Herpfer *et al.*, 1994) and of winonaites of about 4.40–4.54 Ga (Benedix *et al.*, 1998) indicate that these processes occurred very early in solar system history.

CONCLUSION

The winonaite–IAB iron meteorites have complicated textures and chemical–mineralogical features that indicate that the history of the parent body was complex. In an attempt to create the least complicated formation scenario, we explore a hypothesis in which the parent body begins to differentiate, but the differentiation process was cut short (or interrupted) by a catastrophic impact-gravitational reassembly event that caused mixing (scrambling) of disparate lithologies from different formation regions (*e.g.*, surface and interior) in the parent body. Although this hypothesis may not completely explain all properties of these rocks such as the presence of Cr-rich minerals, the atypical chromite compositions, the Na-rich plagioclase, or the absence of basaltic glass, it does explain the mixing of solid silicates with molten metal. It also explains the slow, subsolidus (less than ~700 K) cooling rates (the temperature below which the Widmänstatten structure of the iron meteorites formed) of the buried, reassembled debris.

Acknowledgments–IAB iron meteorite samples were kindly provided by R. S. Clarke, Jr. and G. J. MacPherson (Smithsonian Institution), A. J. Ehlmann (Texas Christian University), J. T. Wasson (Univ. California, Los Angeles), the National Institute of Polar Research, and the Meteorite Working Group. Unpublished data on IAB iron meteorite cooling rates were generously provided by A. Meibom. Helpful discussions were provided by G. J. Taylor, A. Meibom, and J. T. Wasson. Expert technical assistance was provided by T. Servilla and T. Hulsebosch. We thank D. Mittlefehldt, A. Kracher, E. Olsen, and an anonymous reviewer for helpful comments and suggestions that greatly improved the manuscript. The Cray supercomputer used in this investigation was provided by funding from the NASA Offices of Mission to Planet Earth, Aeronautics, and Space Science. This study was supported in part by NASA grants NGT-51652 and NAG 5-4212 (K. Keil, Principal Investigator). This is Hawaii Institute of Geophysics and Planetology publication no. 1121 and School of Ocean and Earth Science and Technology publication no. 5276.

Editorial handling: D. W. Mittlefehldt

REFERENCES

ANTARCTIC METEORITE NEWSLETTER (1986) Johnson Space Center, Houston, Texas, USA. **9,** No.1.

ANTARCTIC METEORITE NEWSLETTER (1988) Johnson Space Center, Houston, Texas, USA. **11,** No. 2.

BENEDIX G. K., LOVE S. G., SCOTT E. R. D., KEIL K., TAYLOR G. J. AND MCCOY T. J. (1996) Catastrophic impact during differentiation of the IAB-winonaite parent asteroid (abstract). *Lunar Planet. Sci.* **27,** 95–96.

BENEDIX G. K., MCCOY T. J., KEIL K., BOGARD D. D. AND GARRISON D. H. (1998) A petrologic and isotopic study of winonaites: Evidence for early partial melting, brecciation, and metamorphism. *Geochim. Cosmochim. Acta* **62,** 2535–2553.

BILD R. W. (1974) New occurrences of phosphates in iron meteorites. *Contrib. Mineral. Petrol.* **45,** 91–98.

BILD R. W. (1977) Silicate inclusions in group IAB irons and a relation to the anomalous stones Winona and Mt. Morris (Wis.). *Geochim. Cosmochim. Acta* **41,** 1439–1456.

BOGARD D., BURNETT D., EBERHARDT P. AND WASSERBURG G. J. (1968) ^{40}Ar-^{40}K ages of silicate inclusions in iron meteorites. *Earth Planet. Sci. Lett.* **3,** 275–283.

BOGARD D., TAKEDA H., MITTLEFEHLDT D. W. AND GARRISON D. (1999) Petrology, ^{39}Ar-^{40}Ar and exposure ages, and chemistry of a gabbro area from the caddo co. IAB iron (abstract). *Lunar Planet. Sci.* **30,** #1253, Lunar and Planetary Institute, Houston, Texas, USA (CD-ROM).

BUCHWALD V. F. (1975) *Handbook of Iron Meteorites*. Univ. California Press, Berkeley, California, USA. 1418 pp.

BUNCH T. E., KEIL K. AND OLSEN E. (1970) Mineralogy and petrology of silicate inclusions in iron meteorites. *Contrib. Mineral. Petrol.* **25,** 297–340.

BUNCH T. E., KEIL K. AND HUSS G. I. (1972) The Landes meteorite. *Meteoritics* **7,** 31–38.

CAFFEE M. W., GOSWANI J. N., HOHENBERG C. M., MARTI K. AND REEDY R. C. (1988) Irradiation records in meteorites. In *Meteorites and the Early Solar System* (eds. J. F. Kerridge and M. S. Matthews), pp. 205–245. Univ. Arizona Press, Tucson, Arizona, USA.

CHOI B-G., OUYANG X. AND WASSON J. T. (1995) Classification and origin of IAB and IIICD iron meteorites. *Geochim. Cosmochim. Acta* **59,** 593–612.

CLAYTON R. N. AND MAYEDA T. K. (1996) Oxygen isotope studies of achondrites. *Geochim. Cosmochim. Acta* **60,** 1999–2018.

COWAN K. A. AND MCCOY T. J. (1998) Mass equivalence and brecciation in the Mt. Padbury mesosiderite (abstract). *Lunar Planet. Sci.* **29,** #1194, Lunar and Planetary Institute, Houston, Texas, USA (CD-ROM).

DAVIS D. R, CHAPMAN C. R., GREENBERG R., WEIDENSCHILLING S. J. AND HARRIS A. W. (1979) Collisional evolution of asteroids: Populations, rotations, and velocities. In *Asteroids* (ed. T. Gehrels), pp. 528–557. Univ. Arizona Press, Tucson, Arizona, USA.

DODD R. T. (1981) *Meteorites: A Petrologic–Chemical Synthesis*. Cambridge Univ. Press, Cambridge, U.K. 368 pp.

DOMINIK B. AND BUSSY F. (1994) Silicate-bearing inclusions in iron-meteorites Caddo County and Zagora. *Archive Des Sciences* **47,** 231-236.

FUCHS L. H. (1969) The phosphate mineralogy of meteorites. In *Meteorite Research* (ed. P. M. Millman), pp. 683–695. D. Reidel, Dordrecht, The Netherlands.

GHOSH A. AND MCSWEEN H. Y., JR. (1998) A thermal model for the differentiation of asteroid 4 Vesta, based on radiogenic heating. *Icarus* **134,** 187–206.

HARTMANN W. K. (1979) Diverse puzzling asteroids and a possible unified explanation. In *Asteroids* (ed. T. Gehrels), pp. 446–479. Univ. Arizona Press, Tucson, Arizona, USA.

HERPFER M. A., LARIMER J. W. AND GOLDSTEIN J. I. (1994) A comparison of metallographic cooling rate methods used in meteorites. *Geochim. Cosmochim. Acta* **58,** 1353–1366.

JAROSEWICH E. (1967) Chemical analysis of seven stony meteorites and one iron with silicate inclusions. *Geochim. Cosmochim. Acta* **31,** 1103-1106.

KEIL K., HAACK H. AND SCOTT E. R. D. (1994) Catastrophic fragmentation of asteroids: Evidence from meteorites. *Planet. Space Sci.* **42,** 1109-1122.

KEIL K., STÖFFLER D., LOVE S. G. AND SCOTT E. R. D. (1997) Constraints on the role of impact heating and melting in asteroids. *Meteorit. Planet. Sci.* **32,** 349–363.

KELLY W. R. AND LARIMER J. W. (1977) Chemical fractionation in meteorites-VII. Iron meteorites and the cosmochemical history of the metal phase. *Geochim. Cosmochim. Acta* **41,** 93–111.

KRACHER A. (1974) Untersuchungen am Landes Meteorit. In *Analyse Extraterrestrischen Materials* (eds. W. Kiesl and H. Malissa, Jr.), pp. 315–326. Springer, New York, New York, USA.

KRACHER A. (1982) Crystallization of a S-saturated Fe,Ni-melt, and the origin of the iron meteorite groups IAB and IIICD. *Geophys. Res. Lett.* **9,** 412–415.

KRACHER A. (1985) The evolution of the partially differentiated planetesimals: Evidence from iron meteorite groups IAB and IIICD. *J. Geophys. Res.* **90 (Suppl.),** C689–C698.

KUBASCHEWSKI O. (1982) *Iron-Binary Phase Diagrams*. Springer, New York, New York, USA. 185 pp.

KULLERUD G. (1963) The Fe-Ni-S system. *Ann. Rep. Geophys. Lab.* **67,** 4055–4061.

LOVE S. G. AND AHRENS T. J. (1996) Catastrophic impacts on gravity dominated asteroids. *Icarus* **124,** 141–155.

MACPHERSON G. J., DAVIS A. M. AND ZINNER E. K. (1995) The distribution of aluminum-26 in the early Solar System—A reappraisal. *Meteoritics* **30,** 365–386

MARSHALL R. R. AND KEIL K. (1965) Polymineralic inclusions in the Odessa iron meteorite. *Icarus* **4,** 461–479.

MASON B. (1967) Extraterrestrial mineralogy. *Am. Mineral.* **52,** 307–325.

MCCOY T. J., SCOTT E. R. D. AND HAACK H. (1993) Genesis of the IIICD iron meteorites: Evidence from silicate-bearing inclusions. *Meteoritics* **28,** 552–560.

MCCOY T. J., EHLMANN A. J., BENEDIX G. K., KEIL K. AND WASSON J. T. (1996) The Lueders, Texas, IAB iron meteorite with silicate inclusions. *Meteorit. Planet. Sci.* **31,** 419–422.

McSween H. Y., Jr., Bennett M. E. III and Jarosewich E. (1991) The mineralogy of ordinary chondrites and implications for asteroid spectrophotometry. *Icarus* **90,** 107–116.

Melosh H. J. and Ryan E. V. (1997) Asteroids: Shattered but not dispersed (note). *Icarus* **129,** 562–564.

Monaghan J. J. (1992) Smoothed particle hydrodynamics. *Ann. Rev. Astron. Astrophys.* **30,** 543–574.

Morse S. A. (1980) *Basalts and Phase Diagrams.* Springer-Verlag, New York, New York, USA. 493 pp.

Niemeyer S. (1979a) I-Xe dating of silicate and troilite from IAB iron meteorites. *Geochim. Cosmochim. Acta* **43,** 843–860.

Niemeyer S. (1979b) ^{40}Ar-^{39}Ar dating of inclusions from IAB iron meteorites. *Geochim. Cosmochim. Acta* **43,** 1829–1840.

Olsen E. J. and Fuchs L. H. (1968) Krinovite, $NaMg_2CrSi_3O_{10}$; a new meteorite mineral. *Science* **161,** 786–787.

Olsen E. J. and Schwade J. (1998) The silicate inclusions of the Ocotillo IAB iron meteorite. *Meteorit. Planet. Sci.* **33,** 153–155.

Olsen E. J., Kracher A., Davis A. M., Steele I. M., Hutcheon I. D. and Bunch T. E. (1999) The phosphates in IIIIAB iron meteorites. *Meteorit. Planet. Sci.* **34,** 285–300.

Onorato P. I. K., Uhlmann D. R. and Simonds C. H. (1978) The thermal history of the Manicouagan Impact Melt Sheet, Quebec. *J. Geophys. Res.* **83,** 2789–2798.

Palme H., Hutcheon I. D., Kennedy A. K., Sheng Y. J. and Spettel B. (1991) Trace element distribution in minerals from a silicate inclusion in the Caddo IAB-iron meteorite (abstract). *Lunar Planet. Sci.* **22,** 1015–1016.

Ramdohr P., Prinz M. and El Goresy A. (1975) Silicate inclusions in the Mundrabilla meteorite (abstract). *Meteoritics* **10,** 477–479.

Robinson K. L. and Bild R. W. (1977) Silicate inclusions from the Mundrabilla iron (abstract). *Meteoritics* **12,** 354–355.

Scott E. R. D. (1972) Chemical fractionation in iron meteorites and its interpretation. *Geochim. Cosmochim. Acta* **36,** 1205–1236.

Scott E. R. D. (1982) Origin of rapidly solidified metal-troilite grains in chondrites and iron meteorites. *Geochim. Cosmochim. Acta* **46,** 813–823.

Scott E. R. D. and Bild R. W. (1974) Structure and formation of the San Cristobal meteorite, other IB irons and group IIICD. *Geochim. Cosmochim. Acta* **38,** 1379–1391.

Scott E. R. D. and Wasson J. T. (1975) Classification and properties of iron meteorites. *Rev. Geophys. Space Phys.* **13,** 527–546.

Stöffler D., Keil K and Scott E. R. D. (1991) Shock metamorphism of ordinary chondrites. *Geochim. Cosmochim. Acta* **55,** 3845–3867.

Takeda H., Baba T., Saiki K., Otsuki M. and Ebihara M. (1993) A plagioclase-augite inclusion in Caddo County: Low-temperature melt of primitive achondrites (abstract). *Meteoritics* **28,** 447.

Takeda H., Mori H., Hiroi T. and Saito J. (1994) Mineralogy of new Antarctic achondrites with affinity to Lodran and a model of their evolution in an asteroid. *Meteoritics* **29,** 830–842.

Takeda H., Yugami K., Bogard D. and Miyamoto M. (1997) Plagioclase-augite-rich gabbro in the Caddo County IAB Iron and the missing basalts associated with iron meteorites (abstract). *Lunar Planet. Sci.* **28,** 1409–1410.

Takeda H., Bogard D. D., Mittlefehldt D. W. and Garrison D. H. (2000) Mineralogy, petrology, chemistry, and ^{39}Ar-^{40}Ar and exposure ages of the Caddo County IAB iron: Evidence for early partial melt segregation of a gabbro area rich in plagioclase-diopside. *Geochim. Cosmochim. Acta* **64,** 1311–1327.

Taylor G. J., Maggiore P., Scott E. R. D., Rubin A. E. and Keil K. (1987) Original structures, and fragmentation and reassembly histories of asteroids: Evidence from meteorites. *Icarus* **69,** 1–13.

Taylor G. J., Keil K., McCoy T., Haack H. and Scott E. R. D. (1993) Asteroid differentiation: Pyroclastic volcanism to magma oceans. *Meteoritics* **28,** 34–52.

Voshage H. (1967) Bestrahlungsalter und Herkunft der Eisenmeteorite. *Z. Naturforsch.* **22a,** 477–506.

Wasson J. T. (1972) Parent-body models for the formation of iron meteorites. *Proc. Intl. Geol. Cong.* **24,** 161–168.

Wasson J. T., Willis J., Wai C. M. and Kracher A. (1980) Origin of iron meteorite groups IAB and IIICD. *Z. Naturforsch.* **35a,** 781–795.

Wlotzka F. and Jarosewich E. (1977) Mineralogical and chemical compositions of silicate inclusions in the El Taco, Camp del Cielo, iron meteorite. *Smithsonian Contrib. Earth Sci.* **19,** 104–125.

Yugami K., Takeda H., Kojima H. and Miyamoto M. (1998) Modal mineral abundances and the differentiation trends in primitive achondrites. *Antarct. Meteorite Res.* **11,** 49–70.